Mon. Not. R. Astron. Soc. **361,** 1165–1172 (2005) doi:10.1111/j.1365-2966.2005.09251.x

Optical and near-infrared spectroscopy of nova V1494 Aquilae 1999 no. 2

U. S. Kamath,[1,2★] G. C. Anupama,[2★] N. M. Ashok,[3★] Y. D. Mayya[4★] and D. K. Sahu[1,2★]

[1]*Centre for Research and Education in Science and Technology, Hosakote 562114, India*
[2]*Indian Institute of Astrophysics, Koramangala, Bangalore 560034, India*
[3]*Physical Research Laboratory, Navrangpura, Ahmedabad 380009, India*
[4]*Instituto Nacional de Astrofisica Optica y Electronica, Apdo Postal 51 y 216, 72000 Puebla, Pue., Mexico*

Accepted 2005 May 24. Received 2005 May 16; in original form 2005 April 13

ABSTRACT

Optical and near-infrared spectroscopic observations of the fast nova V1494 Aquilae 1999 no. 2 covering various phases – early decline, transition and nebular – during the first 18 months of its post-outburst evolution are presented in this paper. During this period, the nova evolved in the $P_{fe}P^{o}_{fe}C_{o}$ spectral sequence. The transition from an optically thick wind to a polar blob–equatorial ring geometry is seen in the evolution of the spectral line profiles. There is evidence of density and temperature stratification in the ejecta. Physical conditions in the ejecta have been estimated based on our observations.

Key words: stars: individual: V1494 Aql – novae, cataclysmic variables.

1 INTRODUCTION

Nova V1494 Aquilae 1999 no. 2 was discovered by Pereira on 1999 December 1.875 at a visual magnitude of 6.0 (Pereira 1999). Spectroscopic observations showed emission lines of the Balmer series, O I, Mg II and Fe II, all having P-Cyg profiles (Ayani 1999; Fujii 1999; Moro, Pizzella & Munari 1999). This confirmed the object to be an 'Fe-II' nova in its early stage. The nova reached a maximum brightness of 4.0 on 1999 December 3.4, followed by a rapid decline with characteristic time-scales of $t_2 = 6.6 \pm 0.5$ d and $t_3 = 16 \pm 0.5$ d, making this a fast nova (Kiss & Thomson 2000). The light curve showed oscillations during the transition phase, between mid-January to 2000 April, which was followed by a smooth decline to 15 mag (Kiyota, Kato & Yamaoka 2004). Early spectral evolution in the optical was reported by Kiss & Thomson (2000) and Anupama, Sahu & Mayya (2001). Spectral evolution in the optical spectroscopy indicates likely continued mass ejection for over 195 d (Ijima & Esenoglu 2003; Eyres et al. 2005). The interstellar extinction to the nova has been estimated to be $E(B - V) = 0.6$ from the equivalent widths of the interstellar absorption components of Na I D1 and D2 (Ijima & Esenoglu 2003). Using this result, the authors have estimated the distance to the nova as 1.6 kpc. We adopt all the above parameters in our discussion and calculations (see Section 4.5).

In this paper, we present multi-epoch optical and near-infrared spectra of nova V1494 Aquilae, obtained over a period of 18 months since outburst at various phases of its evolution.

★E-mail: kamath@crest.ernet.in (USK); gca@iiap.res.in (GCA); ashok@prl.ernet.in (NMA); ydm@inaoep.mx (YDM); dks@crest.ernet.in (DKS)

2 OBSERVATIONS

2.1 Optical

Optical CCD spectra were obtained from the Vainu Bappu Observatory on several nights in 1999 December using the OMR spectrograph at the cassegrain focus of the 2.3-m Vainu Bappu Telescope (VBT). The spectra were obtained at a resolution of 11 Å. FeAr and FeNe spectra were used for wavelength calibration. 58 Aql was used as the spectrophotometric standard star (Hamuy et al. 1994). Spectra were also obtained from the Guillermo Haro Astrophysical Observatory (GHAO) during December 4–7 using the B and C spectrograph on the 2.12-m telescope, at resolutions of 10 and 2 Å. The nova was observed during the nebular phase on two occasions in 2001 (April 29 and May 9) from VBT. All spectra were bias subtracted and flat-field corrected in the standard manner, and the one-dimensional spectra were extracted using the optimal extraction method. The spectra were wavelength calibrated and corrected for instrumental response in the standard manner. All data were analysed using various tasks within IRAF.

The spectra are not corrected for telluric absorption. These features are marked in Fig. 1. The absolute flux level is accurate to 10 per cent. On a relative scale, the emission line fluxes are generally accurate to 10 per cent. However, weaker lines have errors up to 20 per cent, while strong lines like Hβ are accurate to 5 per cent.

2.2 Near-infrared

Near-infrared spectra covering the early decline and transition phases were obtained with PRLNIC, an imager–spectrometer based on a 256 × 256 HgCdTe NICMOS3 array detector, at the cassegrain

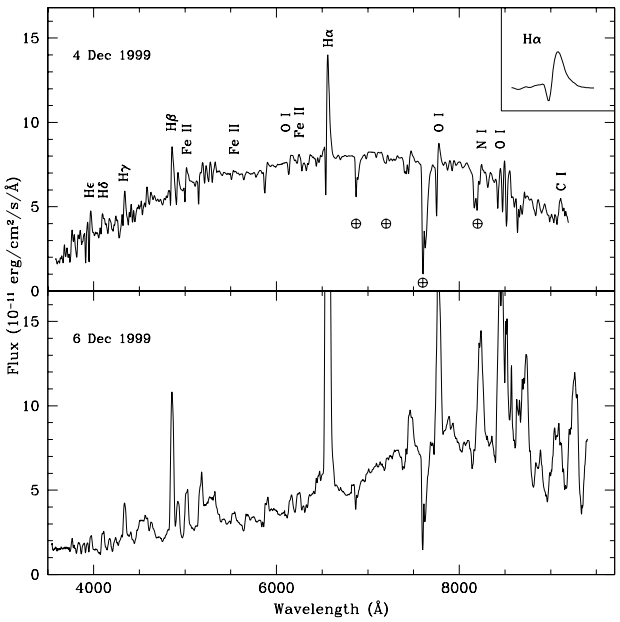

Figure 1. (Top) Spectrum of V1494 Aql in the fireball (pseudophotosphere expansion) phase. Several absorption lines can be seen, and all the emission lines display strong P-Cygni profiles. Terrestrial absorption lines are marked. Inset shows the profile of the Hα line. Prominent lines are labelled.

(Bottom) Spectrum of V1494 Aql displaying the evolution from optically thick to partially optically thin phase. The emission lines have strengthened and the P-Cygni profiles have weakened. Notice the change in the Hα profile.

focus of the 1.2-m telescope of Mt. Abu IR Observatory (MAIRO). To remove the background, spatially offset spectra were obtained by nodding the star along the slit oriented in the north–south direction. One or more spectra were obtained at each position. Nearby standard stars were observed in the same manner. HR 7953, β Tau, δ Aql, HR 5407, λ Ser and α Leo were used as standard stars on different nights. Wavelength calibration was done using the OH skylines. Known stellar absorption features were removed from the standard star spectra, and the nova spectrum was then divided by this. The result was multiplied by the spectrum of a blackbody of temperature commensurate with the spectral type of the standard star. This process removes the effects of atmospheric absorption and instrumental response in the wavelength regions common to the nova and standard star spectra; the nova spectra have slightly different spectral coverage at different epochs. The data were reduced using standard procedures available within IRAF. The fluxes are on a relative scale and accurate to around 10 per cent.

Table 1 gives the details of both optical and near-infrared observations. Fluxes of optical emission lines seen in the early decline and nebular phases are given in Tables 2 and 3, respectively.

3 EVOLUTION OF THE SPECTRA

Nova spectra undergo different phases of evolution depending on the physical conditions of the outflowing gas and temperature of the central remnant. A nova is initially seen as an optically thick fireball, with numerous absorption lines and hardly any emission lines. As the ejecta expands outwards and becomes optically thin with time, numerous emission lines begin to appear. A high-ionization coronal phase is reached in some novae. Eventually, the nova returns to its pre-outburst state.

3.1 Fireball phase

Our first spectrum was obtained on 1999 December 4 at near-maximum. This spectrum (Fig. 1, top panel) displays the fireball phase of the nova explosion. Many members of the Hydrogen Balmer series, right up to Balmer 21, can be seen along with several lines of O I. Signature of the outflowing optically thick wind can be seen as P-Cyg profiles on all these lines. Numerous lines of Fe II, N I, Mg I and C I are also present, although the P-Cyg profiles of some of them are not apparent due to blending with adjacent lines. The absorption components of some lines like the Ca II IR triplet are much stronger than the emission. The absorption velocities lie in the range of 1000–1500 km s^{-1}. Thus, the spectrum is that of optically thick gas flowing outwards from the central source. There possibly are some warm, dense packets of gas in the outflowing material.

3.2 Early decline and transition phase

In the early decline phase of novae, the P-Cygni profiles disappear and the lines acquire a more rounded emission peak. This transition

Table 1. Log of observations.

Date	Coverage	Resolution	Observatory	Instrument
Optical spectra				
1999 December 4	4000–9000 Å	10 Å	GHAO	B&C
1999 December 5	4000–9000 Å	2 Å	GHAO	B&C
1999 December 6–7	4000–9000 Å	10 Å	GHAO	B&C
1999 December 6–7	3700–9500 Å	11 Å	VBT	OMR
1999 December 9–10	4000–9500 Å	11 Å	VBT	OMR
1999 December 15–16	4000–9500 Å	11 Å	VBT	OMR
1999 December 23	4500–7000 Å	11 Å	VBT	OMR
1999 December 25	4000–9000 Å	11 Å	VBT	OMR
2001 April 29	4000–8000 Å	11 Å	VBT	OMR
2001 May 9	4800–9400 Å	11 Å	VBT	OMR
Near-infrared spectra				
1999 December 5	1–2.5 μm	2×10^{-3} μm	MAIRO	PRLNIC
1999 December 7	1–2.5 μm	2×10^{-3} μm	MAIRO	PRLNIC
1999 December 31	1–2.5 μm	2×10^{-3} μm	MAIRO	PRLNIC
2000 February 11	1–2.5 μm	2×10^{-3} μm	MAIRO	PRLNIC
2000 March 1	1–2.5 μm	2×10^{-3} μm	MAIRO	PRLNIC

Table 2. Line identification and observed fluxes relative to Hβ in the early decline phase. Fluxes with higher errors are marked with a colon. See the text for a discussion of the errors.

λ (Å)	Line id	1999 December				
		6	7	10	16	23
3770	Balmer 11	0.02:	0.01:			
3835	Balmer 9	0.06	0.02:			
3889	Balmer 8	0.05	0.03:			
3933	Ca II K(1)	0.04	0.02:			
3970	Ca II H(1) + Hϵ	0.10	0.06			
4101	Hδ	0.14	0.09		0.14	
4173	Fe II(27)	0.01:	0.06		0.07	
4233	Fe II		0.08		0.05	
4340	Hγ	0.22	0.16	0.03:	0.13	
4351	Fe II (27)		0.03:			
4471	He I ?	0.02:	0.04			
4556	Fe II	0.10	0.09			
4584	Fe II(38)	0.08	0.07			
4635	Fe II	0.09	0.09	0.03:		
4649	O II	0.04	0.05	0.03:	0.15	0.21
4861	Hβ	1.00	1.00	1.00	1.00	1.00
4924	Fe II(42)	0.27	0.21	0.18	0.19	0.06
5018	Fe II	0.35	0.33			
5169	Fe II + Mg I	0.12	0.56	0.09	0.10	
5176	N II + Mg I					0.17
5184	Mg I	0.24		0.13	0.13	
5275	Fe II (49) + (84)			0.05		
5316	Fe II (49)			0.01:		
5363	Fe II(48)	0.10		0.04	0.03:	
5425	Fe II	0.04	0.03:			
5535	Fe II(55) + N II	0.10	0.10			
5680	N II(3)	0.08	0.08	0.15		0.30
5755	[N II](3)	0.05	0.07	0.10		0.66
5876	He I ?	0.04				
5909	Fe II	0.12		0.14	0.18	0.23
5942	N II(28)	0.07	0.13			
5991	Fe II(46)	0.04	0.04	0.12		0.28
6084	Fe II(46)	0.03:				
6157	O I	0.15	0.14	0.08	0.06	0.06
6243	Fe II + N II	0.17	0.17	0.05		
6300	[O I]	0.03:		0.04		0.10
6363	[O I]			0.04		0.08
6563	Hα	5.92	8.0	3.55	5.86	13.2
7774	O I	1.53	2.87	0.47	0.37	
8232	O I (34) + Mg II(7)	1.34	2.00	0.24	0.29	
8446	O I	2.57	4.63	1.18	1.82	
8662	Ca II (2) + Pa 13		2.26			
8863	Paschen 11		0.87			
9042	N I(15)	0.45	0.75	0.10	0.12	
9112	C I	0.27				
9229	Paschen 9			0.33	0.44	
9264	O I	1.23	2.55			
9405	C I (9)		0.84			
9546	Paϵ		0.52			
	$F_{H\beta}$ (10^{-9} erg cm^{-2} s^{-1})	3.55	2.88	1.96	1.37	0.65

can be seen in our spectra obtained on 1999 December 6 (Fig. 1, bottom panel). Polarization observations by Kawabata et al. (2001) during this period revealed a drastic change in the position angle of the intrinsic polarization (from 65° to 140°). They have interpreted this in terms of an optical depth effect or a geometric change in the nova wind. A combination of both these effects are likely to be responsible for this change.

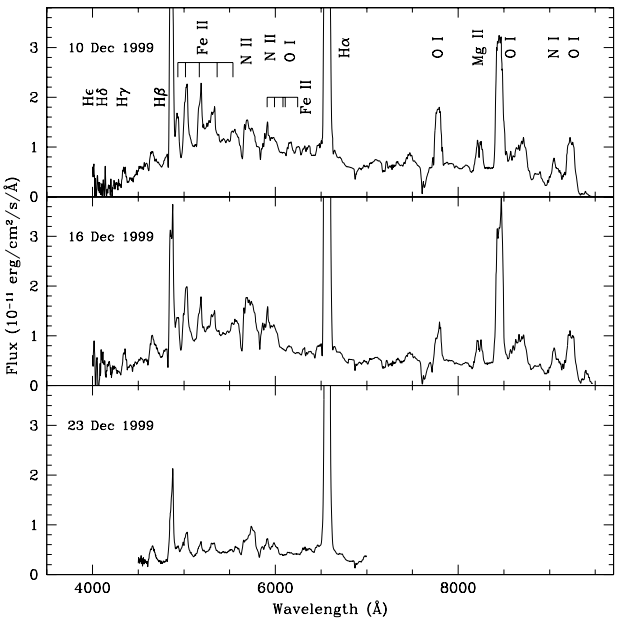

Figure 2. Spectra of V1494 Aql in the early decline phase. The gradual hardening of the spectrum is reflected in the weakening of Fe II lines and the sustained strength of lines of higher ionization.

Subsequent optical spectra displayed in Fig. 2 show typical characteristics of Fe-II novae – numerous Fe II and N II lines – along with prominent lines of Hα, Hβ and O I. The emission lines show P-Cyg profiles on the first few days and become more rounded subsequently. An optically thin wind gives a rounded emission peak, while an optically thin shell produces a more rectangular line profile (Williams 1992, and references therein). The profile of the Hα line shown in Fig. 3 clearly demonstrates the prominence of the wind and shell components at different times. Initially, it shows a strong P-Cyg absorption and is representative of an optically thick wind. Later, it shows characteristic of optically thin wind, and eventually

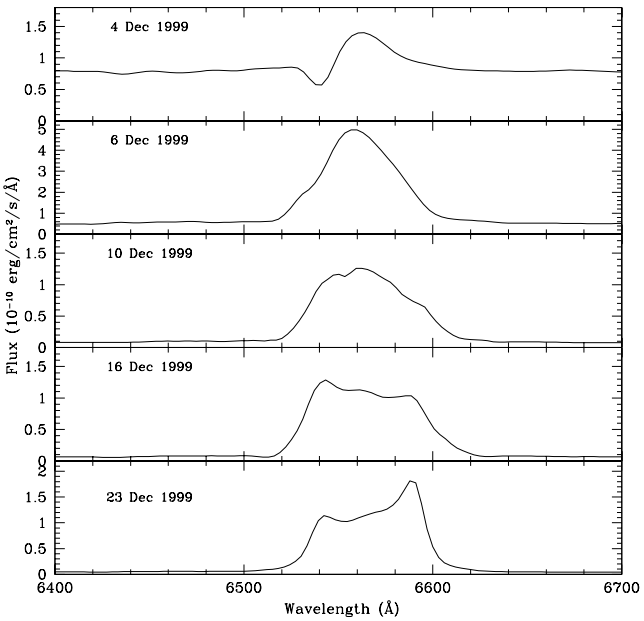

Figure 3. Evolution of the Hα line showing the transition from an optically thick wind to a polar blob–equatorial ring geometry.

shows the typical saddle shape of the polar blob–equatorial ring geometry of the ejected shell (see Section 4.1). The hardening of the spectrum with time can be seen in the weakening of the Fe II and N II lines, and the continuing strength of the O I 8446-Å line. Some lines like He I (4471, 5876 Å) and [O I] (6300, 6363 Å) are clearly seen in emission, only on some days. The FWHM (full width at half-maximum) of the Hβ line lies in the range of 2280–2875 km s^{-1} in this period, with no apparent secular change.

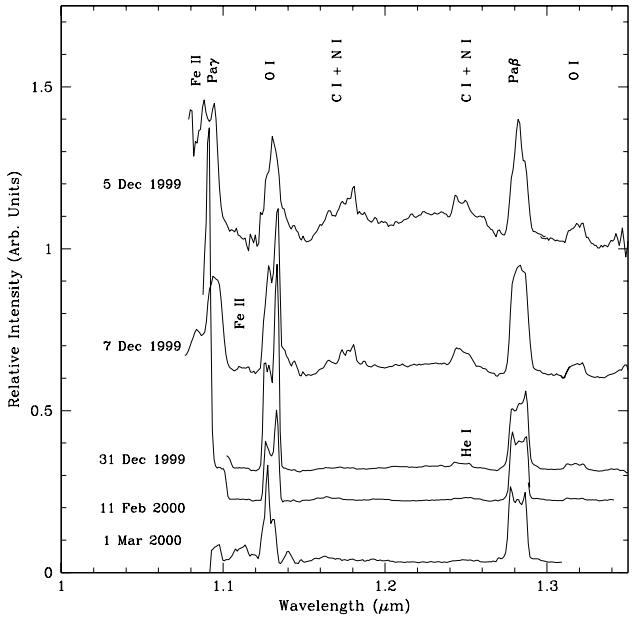

Figure 4. *J*-band spectra of V1494 Aql in the early decline and transition phases. Spectra obtained on different nights have been scaled and shifted for clarity. Increasing ionization level of the ejecta is reflected in the gradual weakening of carbon and nitrogen lines and appearance of helium lines.

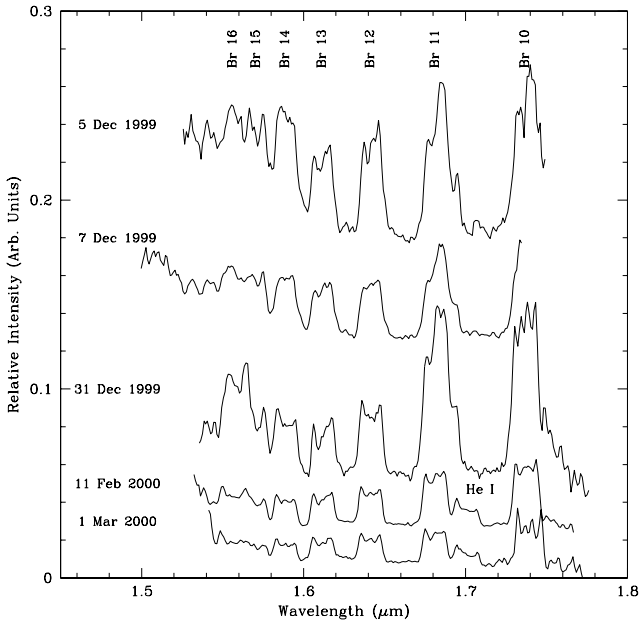

Figure 5. *H*-band spectra of V1494 Aql in the early decline and transition phases. This spectral region mainly covers the hydrogen Brackett series, but some unidentified lines (see text for details) and the He I 1.7-μm line can also be seen.

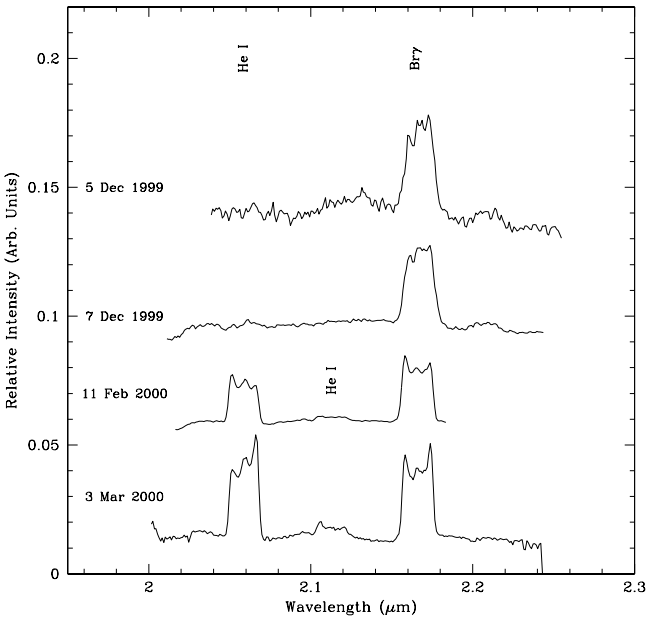

Figure 6. *K*-band spectra of V1494 Aql. The increasing level of ionization is apparent in the emergence and strengthening of the helium lines.

Near-infrared spectra obtained on various days are shown in Figs 4–6. In each of these panels, the spectra have been offset from each other and scaled for illustrative purposes. Lines of hydrogen (Paschen and Brackett series) and oxygen are prominent in the 1999 December 5 spectra. The *J* band has several lines due to C I and N I. The overall spectrum is typical of an Fe-II nova in the very early decline stage. None of the lines show significant P-Cygni profiles, suggesting that the nova ejecta had become optically thin in the near-infrared as early as day 2. The increasing level of ionization of the ejecta is reflected in the gradual decrease in the line strengths of Fe II, C I and N I, and the appearance of various lines of He I. The strong line near 1.08 μm seen on 1999 December 5 is likely to be Fe II, as is corroborated by its reduced strength 2 d later. The He I lines at 1.252, 1.700 and 2.058 μm are seen starting from, respectively, 28, 70 and 70 d since maximum. The He I lines of 2000 March are very strong. The FWHMs of the hydrogen and helium lines lie in the range 2100–2800 km s^{-1}. Again, no temporal trend can be seen.

3.3 Late-stage nebular spectra

V1494 Aql showed fairly strong nebular lines and weak coronal lines at around 65 and 80 d, respectively (Ijima & Esenoglu 2003), during the transition phase. Infrared coronal lines seen in 2000 July (day 226), along with lines of H I, He I and He II (Venturini et al. 2000) show that the nova ejecta had zones of low or no ionization coeval with the highly ionized zone. Optical spectra (Arkhipova, Burlak & Esipov 2002; Ijima & Esenoglu 2003) show that by 2000 September (day $\sim$ 280) the coronal lines had strengthened considerably, while the low-ionization lines, such as He I, had weakened significantly. Our spectra (see Figs 7 and 8) show no He I lines, indicating that the helium has been completely ionized by day $\sim$510. Similarly, the absence of [O I] 6300-Å line implies that the zone where neutral oxygen was present earlier also has been ionized. Both spectra show many lines of highly ionized iron.

CHANDRA observations show that the nova had become a super-soft X-ray source by 2000 August (Starrfield et al. 2000). This is the signature of the energy emitted by hydrostatic hydrogen burning (of

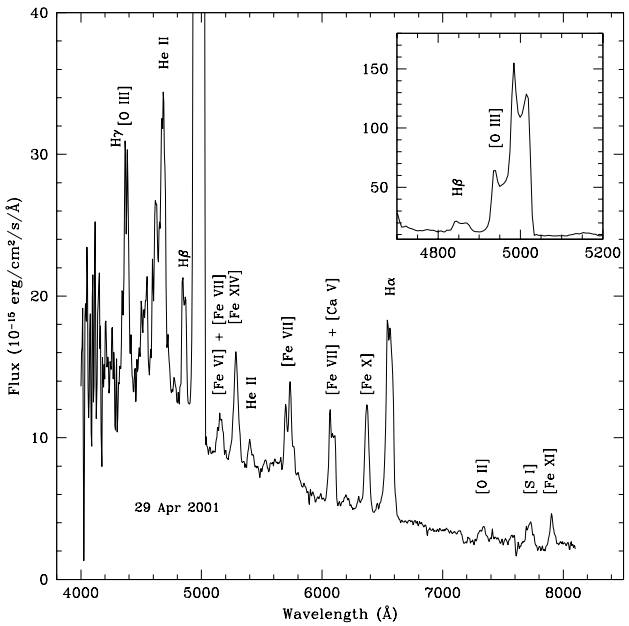

Figure 7. Spectrum of V1494 Aql in the coronal phase obtained in 2001 April. Many lines of highly ionized iron can be seen. Inset shows the region around the [O III] lines.

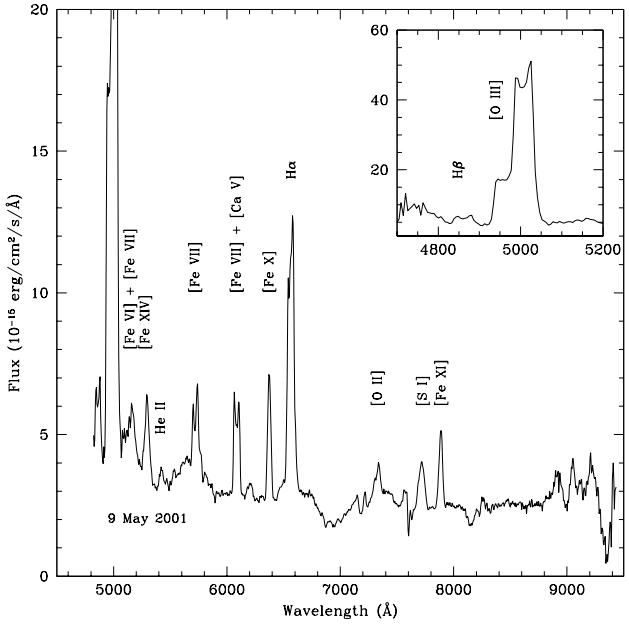

Figure 8. Spectrum of V1494 Aql in the coronal phase obtained in 2001 May. The emission lines have strengthened further showing a continued hardening of the spectrum. Inset shows the region around the [O III] lines.

the unejected matter) on the surface of the white dwarf. The 2001 April spectrum (see Fig. 7) shows that the lines of highly ionized iron have sharp, single-peaked profiles. The nebular lines are double peaked and show similar structure as that of the Balmer lines. This suggests that the coronal lines could be arising in a region different (possibly closer to the hot white dwarf) from that of the nebular (and other) lines. This conforms to the model of a nova shell presented by Saizar & Ferland (1994), wherein the ejecta consist of warm

Table 3. Line identification and observed fluxes relative to Hβ in the coronal phase. The fluxes are accurate up to 10 per cent.

λ (Å)	Line id	2001	
		April	May
4340 + 4363	Hγ + [O III]	1.90	
4686	He II	2.96	
4861	Hβ	1.00	1.00
4959 + 5007	[O III]	23.06	20.49
5159	[Fe VI] + [Fe VII]	0.31	
5303	[Fe XIV]	1.04	0.92
5411	He II	0.22	
5720	[Fe VII]	0.95	1.30
6087	[Fe VII] + [Ca V]	1.0	1.23
6310	[S III]	0.05	0.24
6374	[Fe X]	0.92	1.11
6563	Hα	2.68	4.02
7330	[O II]	0.17	0.43
7727	[S I]	0.25	0.69
7891	[Fe XI]	0.25	0.75
9069	[S III]		0.21
	$F_{H\beta}$ (10^{-13} erg cm $^{-2}$ s^{-1})	3.44	1.41

($T \sim 10^4$ K), dense clouds, embedded in a hot ($T \sim 10^6$ K), tenuous gas. The two phases are photoionized by the hard white dwarf continuum, and the warm phase is further photoionized by the free–free continuum generated in the hot gas. Thus, the nebular spectra require some kind of non-uniform (in temperature and density) shell structure to explain the observed range of ionization.

In Section 4.5, we have derived values for the physical conditions of the ejecta in this stage.

3.4 Spectral evolutionary sequence

The Tololo classification system for novae has been evolved to define the temporal evolution of a nova spectrum (Williams et al. 1991; Williams, Phillips & Hamuy 1994). Every nova can be assigned an evolutionary sequence according to the various phases and subclasses for each phase that are observed in the optical spectra. In the early decline phase (1999 early-December), permitted lines of Fe II were the strongest non-Balmer lines; hence, the spectral classification of the nova during this phase is P_{fe}. Also, the O I 8446-Å line remained stronger than Hβ, while the nova was still in the permitted line phase. Hence, a classification of P^o_{fe} can be assigned. If [Fe X] 6375-Å emission is clearly present and stronger than [Fe VII] 6087 Å, the nova spectrum is considered to be in the coronal phase, regardless of any other line strengths. This is the case during 2001 April. The strongest non-Balmer line in this spectrum is [O III] 5007 Å, and therefore the nova is in the C_o phase. Thus, the evolutionary sequence for V1494 Aql is $P_{fe}P^o_{fe}C_o$.

4 DISCUSSION

4.1 Ejecta geometry

Nova shells are not uniform, but show considerable structure because of the clumpy nature of the ejecta (e.g. Anupama & Prabhu 1993). A double-peaked, saddle-shaped emission profile is the signature of emission from a shell of material, which has an equatorial-ring, polar-cone/blob morphology (Hutchings 1972). Substructures

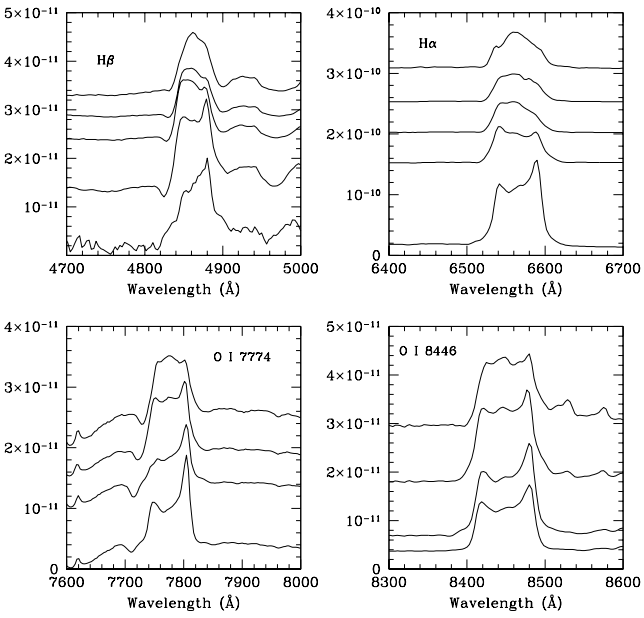

Figure 9. Temporal evolution of some optical emission line profiles in spectra obtained during 1999 early- (top) and late-December (bottom). The spectra have been shifted or scaled for illustrative purposes.

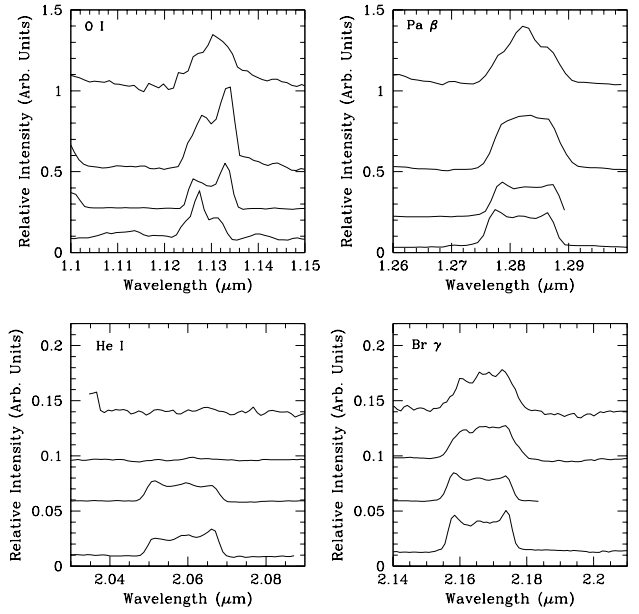

Figure 10. Evolution of some near-infrared emission line profiles seen in the early (1999 December – top) to the later (2000 March – bottom) spectra. The spectra have been shifted or scaled for illustrative purposes.

within the shell manifest themselves as multiply peaked spectral lines (Gill & O'Brien 1999). Nova V1494 Aql showed triangular lines in the initial phases (see Figs 9 and 10). They broadened and acquired a more rectangular, multipeaked profile with time. The velocities deduced from emission peaks range from 500 to 1200 km s^{-1}, although the O I lines show higher velocity components of up to 2500 km s^{-1}. Spectropolarimetric observations of this nova have shown that an asymmetric geometry was present even prior to maximum brightness (Kawabata et al. 2001). At around 10 d after maximum light, rapidly variable components of polarization were observed, and their contribution increased with time. This is due to clumping in ejection near the nova. A radio image obtained using Multi-Element Radio-Linked Interferometer Network (MERLIN) on day 136 shows that the ejecta continued to have this clumpy structure (Eyres et al. 2005).

The line profiles (Figs 9 and 10) seen in the later decline phases are similar to those seen in nova shell models having shell inclination angles between 60° and 90° (Gill & O'Brien 1999). Kiss & Thomson (2000) infer that the shell is seen edge-on, whereas Eyres et al. (2005) favour a low inclination angle. It is to be noted that similar profiles may be produced by different parameters of inclination angles, ellipticities and positions of rings (Gill & O'Brien 1999). In the absence of detailed modelling, we can only say that the nova spectra reflect the structure (equatorial ring–polar ring/cap) of the shell. As seen in the insets in Figs 7 and 8, the nebular line profiles show changes in the red–blue asymmetry during the two epochs, reflecting the fact that shell shaping is continuing even at this late stage.

4.2 Lyβ fluorescence

A striking feature of the spectra is the presence of strong lines of oxygen. The 1.128-μm line is much stronger than the 1.316-μm line on all days. Also, the 8446-Å line is stronger than would be expected from recombination alone, which should produce $F_{8446}/F_{H\alpha} \leqslant 10^{-4}$ (Rudy, Rossano & Puetter 1989). The 1.128-μm line is predominantly produced from fluorescent excitation of O I by Lyβ (Bowen fluorescence). This is also the dominant mechanism for the 8446-Å line. The main implication of strong O I lines generated by Lyβ fluorescence is the existence of a region or regions where a sizeable fraction of the O and H is neutral, but where a high Lyβ flux density is also present. Such regions are dense, warm and quite thick optically in the Lyman lines.

4.3 Unidentified lines

Several novae have shown unidentified lines at 0.8926, 1.1110, 1.1900, 1.5545 and 2.0996 μm [e.g. V4633 Sgr (Lynch et al. 2001), V723 Cas (Rudy et al. 2002), CI Aql (Lynch et al. 2004)]. They first appear about the same time as the He II lines and generally persist till the coronal phase. Thus, they are of medium-to-high excitation and require relatively low electron densities for appearance (Lynch et al. 2004). Near-infrared spectra of V1494 Aql display at least two of these lines – 1.1110 and 1.5545 μm. The Brackett 16 line appears unusually strong in the 1999 December 31 spectrum, and it could be blended with the unidentified line at 1.5545 μm. The shoulder on Paγ line on 2000 Feb 11 could be the 1.111-μm line. There are a few other unidentified lines that are seen only in some novae. For example, the lines at 1.6983 μm (V2487 Oph – Lynch et al. 2000) and 1.770 μm (V838 Her – Harrison & Stringfellow 1994). The 1.6983-μm line is seen in V1494 Aql on 1999 December 31 as a blend with the Brackett 11 line, which appears unusually strong. The unidentified line at 1.770 μm is seen in the 2000 March 1 spectrum.

4.4 Ejecta ionization

The ejecta of V1494 Aql displayed only low-excitation lines in the first month following outburst. He I emission lines were not seen in our 1999 December spectra (only the He I 1.252-μm line is seen in the 1999 December 31 spectrum), indicating that the

level of ionization was less than 25 eV. The appearance and rapid rise of the He I lines in 2000 February and March (see Figs 5 and 6) suggest that the ejecta was evolving to a higher excitation state in this period. By 2000 July, the ejecta ionization had reached more than 329 eV (Venturini et al. 2000). However, lines of lower ionization were also seen, suggesting that there were still some denser, cooler zones within the clumpy ejecta. About 17 months after the outburst, such zones hardly existed and the ejecta were almost completely ionized, as can be seen in Fig. 7. Increased emission line strengths in 2001 May (see Fig. 8) suggest a further hardening of the nova spectrum.

4.5 Physical parameters of the ejecta

Emission line fluxes corrected for extinction enable us to determine physical conditions in the ejecta. We have used the nebular stage spectra because they are ideal for abundance estimates.

Since the standard nebular lines used for density estimate are not available in our data, we use the Hβ luminosity to estimate the electron number density, N_e. The volume of the line-emitting region is estimated assuming the shell to be spherical, with a filling factor of 0.01 (Ijima & Esenoglu 2003 obtained a value of 0.016 in 2000 June), and uniformly expanding with a velocity of 2500 km s^{-1}. The electron temperature, T_e, in this region is assumed to be 1.5×10^4 K. Using these simplistic assumptions, the N_e is found to be $1.1(\pm 0.06) \times 10^5$ cm^{-3}. Only the uncertainty in flux is considered for calculating the error. As mentioned in Section 4.1, the shell is aspherical and there could exist several velocity components. From the derived N_e we estimate the mass of hydrogen in the ejecta, M_H, to be 6×10^{-6} M$_\odot$. The total ejecta mass would be higher than this value.

Assuming that all the helium is ionized, the helium abundance by number is estimated using the He II 4686/Hβ ratio. The hydrogen and He II emissivities are from Hummer & Storey (1987). The helium abundance of V1494 Aql is found to be 0.24, and is similar to that observed in other novae such as V1425 Aql (Kamath et al. 1997).

We have used the NEBULAR package (Shaw & Dufour 1995) within IRAF to calculate T_e in the zone of nebular lines and ionic abundances. T_e, as determined using [O III] line fluxes, is $1.0(\pm 0.02) \times 10^5$ K. The ionic abundances with respect to H^+ are calculated assuming that both the emission lines – nebular and Hβ – arise in regions with the same T_e and N_e. This assumption is not strictly true (e.g. the O^+ ion requires $T_e \leqslant 2 \times 10^4$ K), but provides a first-order estimate of the abundances in the ejecta. The abundances of O^+, O^{2+} and S^{2+} are shown in Table 4. As mentioned in Sections 3.3, 4.1 and 4.4, there is a density, as well as temperature, stratification in the ejecta. In the absence of detailed modelling, the values in Table 4 are considered to be representative of the conditions in the ejected material.

Table 4. Physical conditions in the ejecta during the nebular phase.

Parameter	Value	Line used
N_e	$1.1\ (\pm 0.06) \times 10^5$ cm^{-3}	Hβ
M_H	6×10^{-6} M$_\odot$	Hβ
T_e	$1.0\ (\pm 0.02) \times 10^5$ K	[O III]
He/H	0.24 ($\pm$0.06)	He II 4686 Å
$N(O^+)/N(H^+)$	1.45×10^{-5}	[O II] 7330 Å
$N(O^{2+})/N(H^+)$	1.57×10^{-6}	[O III] 4959+5007 Å
$N(S^{2+})/N(H^+)$	7.5×10^{-8}	[S III] 6312 Å
$N(S^{2+})/N(H^+)$	3.4×10^{-7}	[S III] 9069 Å

The early spectra show numerous lines of neutral oxygen, carbon and nitrogen. Lines such as O I 9264 Å and N I 9042 Å are produced solely by recombination. This indicates an abundance enhancement of these elements. Also, since the mechanism of Lyβ fluorescence is very strong and persistent for a long time, it indicates the possible presence of a region of fairly high oxygen abundance. Therefore, the CNO abundances seem to be enhanced. This is broadly in line with present nova theories (see Hernanz 2005, for a recent review).

5 REMARKS

We have presented optical and near-infrared spectra of the fast nova V1494 Aquilae 1999 no. 2 in the early decline, transition and nebular phases, covering 18 months since outburst. Based on our data and observations reported in literature, the following picture emerges.

Nova V1494 Aql was a fast nova that ejected matter asymmetrically at velocities of 1000–2500 km s^{-1}. The ejected matter was optically thick initially, but partial thinness set in soon. The ejecta displayed low-ionization levels during the first month after outburst. Higher ionization lines were evident after about day 65. At about 17 months after outburst, the ejecta were largely ionized and showed strong coronal lines. The clumpy nature of the ejecta was evident in polarization observations, spectral line profiles, nebular lines and the MERLIN radio image. The nebular spectra present evidence of temperature and density stratification within the ejecta. The calculated elemental and ionic abundances in the ejecta are similar to those found in other novae.

ACKNOWLEDGMENTS

We thank all staff members of the respective observatories for help during the observations. Research work at Physical Research Laboratory is funded by the Department of Space, Government of India. IRAF is distributed by the National Optical Astronomy Observatories, which are operated by the Association of Universities for Research in Astronomy, Inc., under cooperative agreement with the National Science Foundation.

REFERENCES

Anupama G. C., Prabhu T. P., 1993, MNRAS, 263, 335
Anupama G. C., Sahu D. K., Mayya Y. D., 2001, BASI, 29, 375
Arkhipova V. P., Burlak M. A., Esipov V. F., 2002, Astron. Lett., 28, 100
Ayani K., 1999, IAUC 7324
Eyres S. P. S., Heywood I., O'Brien T. J., Ivison R. J., Muxlow T. W. B., Elkin V. G., 2005, 358, 1019
Fujii M., 1999, IAUC 7324
Gill C. D., O'Brien T. J., 1999, MNRAS, 307, 677
Hamuy M, Suntzeff N. B., Heathcote S. R., Walker A. R., Gigoux P., Phillips M. M., 1994, PASP, 106, 566
Harrison T. E., Stringfellow G. S., 1994, ApJ, 437, 827
Hernanz M., 2005, in Hameury J.-M., Lasota J.-P., eds, The Astrophysics of Cataclysmic Variables and Related Objects, Proc. ASP Conf. Vol. 330. Astron. Soc. Pac., San Francisco, p. 265
Hummer D. G., Storey P. J., 1987, MNRAS, 224, 801
Hutchings J. B., 1972, MNRAS, 158, 177
Iijima T., Esenoglu H. H., 2003, A&A, 404, 997
Kamath U. S., Anupama G. C., Ashok N. M., Chandrasekhar T., 1997, AJ, 114, 2671
Kawabata K. S. et al., 2001, ApJ, 552, 782
Kiss L. L., Thomson J. R. 2000, A&A, 355, L9
Kiyota S., Kato T., Yamaoka H., 2004, PASJ, 56, S193

Lynch D. K., Rudy R. J., Mazuk S., Puetter R. C., 2000, ApJ, 541, 791
Lynch D. K., Rudy R. J., Venturini C. C., Mazuk S., 2001, AJ, 122, 2013
Lynch D. K., Wilson J. C., Rudy R. J., Venturini C., Mazuk S., Miller N. A., Puetter R. C., 2004, AJ, 127, 1089
Moro D., Pizzella A., Munari U., 1999, IAUC 7325
Pereira A., 1999, IAUC 7323
Rudy R. J., Rosano G. S., Puetter R. C., 1989, ApJ, 346, 799
Rudy R. J., Venturini C. C., Lynch, D. K., Mazuk S., Puetter R. C., 2002, ApJ, 573, 794
Saizar P., Ferland G. J., 1994, ApJ, 425, 755
Shaw R. A., Dufour R. J., 1995, PASP, 107, 896
Starrfield S. et al., 2000, BAAS, 32, 1253
Venturini C., Rudy R. J., Lynch D. K., Mazuk S., Puetter R. C., Armstrong T., 2000, IAUC 7490
Williams R. E., 1992, AJ, 104, 725
Williams R. E., Hamuy M., Phillips M. M., Heathcote S. R., Wells L., Navarrete M., 1991, ApJ, 376, 721
Williams R. E., Phillips M. M., Hamuy M., 1994, ApJS, 90, 297

This paper has been typeset from a TEX/LATEX file prepared by the author.